This full text paper was peer-reviewed at the direction of IEEE Instrumentation and Measurement Society prior to the acceptance and publication

Scale-Adaptive Pothole Detection and Tracking from 3-D Road Point Clouds

Rigen Wu, Jiahe Fan, Libo Guo, Lei Qiao,
M. Usman Maqbool Bhutta, Brett Hosking, Sergey Vityazev, Rui Fan

2021 IEEE International Conference on Imaging Systems and Techniques (IST) | 978-1-7281-7371-9/21/$31.00 ©2021 IEEE | DOI: 10.1109/IST50367.2021.9651423

***Abstract*—3-D road surface modeling has become an essential part of modern algorithms for road pothole detection when 3-D road point clouds are available. This paper introduces a scale-adaptive road pothole detection and tracking framework. It first fits a quadratic surface to the 3-D road point cloud, generated using GPT-SGM, a state-of-the-art disparity estimation algorithm. The surface modeling process also incorporates the normal vector information, obtained by three-filters-to-normal (3F2N), an ultra-fast and accurate surface normal estimator. By comparing the actual and modeled 3-D road surface point clouds, the pothole point clouds can be extracted. Finally, the discriminative scale space tracking (DSST) algorithm is utilized to track the detected potholes in a sequence of successive video frames. Extensive experimental results demonstrate the robustness of our proposed road pothole detection and tracking framework both qualitatively and quantitatively.**

I. Introduction

A. Background

Potholes are deep depressions on the road surface caused by erosion and wear [1]. They are typically detected and reported by certified inspectors or structural engineers [2], [3]. This process is, however, not only hazardous for the personnel but also cumbersome and time-consuming [4]–[6]. Additionally, the pothole detection results are always subjective because they depend entirely on the experience of the individual personnel [7], [8]. Therefore, there has been an ever-increasing need for automated road pothole detection systems [9].

In recent years, laser scanning equipment has been extensively used for 3-D road information acquisition [10], while other technologies, *e.g.*, passive sensing, are underutilized [11], [12]. However, such laser scanners mounted on digital inspection vehicles (DIVs) are costly and cannot be adapted for other vehicles [13]. Recently, major advancements have been achieved in the field of computer vision regarding dense disparity image estimation [14]. A stereo vision system can now reconstruct the 3-D geometry structure of road surfaces with an accuracy of over 3 mm [15], [16]. Therefore, the trend is to equip vehicles with portable, inexpensive, and durable sensors, such as stereo cameras, for 3-D road data acquisition and pothole detection [17].

Rigen Wu is with the School of Civil Engineering, Inner Mongolia University of Technology, Hohhot 010051, P. R. China (email: wrg6370@outlook.com).

Jiahe Fan is with the School of Information and Electronics, Beijing Institute of Technology, Beijing 100811, P. R. China (email: jhxfan@ieee.org).

Libo Guo is with Taiyuan IntelliVision Co. Ltd., Taiyuan 030006, China (email: glbbobo@outlook.com).

Lei Qiao is with the State Key Laboratory of Ocean Engineering and the School of Naval Architecture, Ocean and Civil Engineering, Shanghai Jiao Tong University, Shanghai, 200240, P. R. China (e-mail:qiaolei@sjtu.edu.cn).

M. Usman Maqbool Bhutta is with the Department of Mechanical and Automation Engineering, the Chinese University of Hong Kong, Hong Kong SAR, P. R. China (email: usmanmaqbool@outlook.com).

Brett Hosking is with Arm, Manchester M1 3HU, United Kingdom (email: brett.hosking@arm.com).

Sergey Vityazev is with the Department of Telecommunications and Radio Engineering Foundations, Ryazan State Radio Engineering University, Ryazan 390005, Russia (email: vityazev.s.v@ieee.org).

Rui Fan is with the Department of Control Science and Engineering, Tongji University, Shanghai 201804, P. R. China (email: rui.fan@ieee.org).

Rigen Wu and Jiahe Fan contributed equally to this work.

B. State of the art in Road Pothole Detection

Existing road pothole detection approaches can either be classified as 2-D image analysis-based or 3-D road surface modeling-based [17]. The former typically apply traditional image processing algorithms (*e.g.*, morphological filtering, thresholding, *etc.*) and/or machine/deep learning algorithms (*e.g.*, convolutional neural networks [18]–[26] for semantic segmentation or object detection) to extract a region of interest (RoI) from the given 2-D road image, such as an RGB image or a depth/disparity image [27]–[35]. On the other hand, the 3-D road surface modeling-based approaches have become popular in recent years [36], [37]. The work presented in [38] is a typical example. It first reconstructs the 3-D road geometry structure from stereo road images. A quadratic 3-D road surface was then fitted to the reconstructed 3-D road surface. By comparing the interpolated and original 3-D road surfaces, the pothole regions can be detected. Recently, [17] presented a hybrid road pothole detection algorithm that combines both 2-D image analysis and 3-D road surface modeling. It first proposes a novel disparity image transformation algorithm, which can better distinguish between damaged and undamaged road areas. The transformed disparity image is then segmented using Otsu's thresholding algorithm [39]. The disparities in the undamaged road areas are subsequently interpolated into a quadratic road surface, where the road surface normals are also incorporated into the surface interpolation process. The road potholes are then detected by comparing the difference between the interpolated and original disparity maps.

C. System Design

The aforementioned 3-D road surface modeling process is very time-consuming. Therefore, in this paper, we first use random sample consensus (RANSAC) to improve both the robustness and efficiency of road surface modeling, where the surface normal information is also incorporated to eliminate outliers and it is acquired using three-filters-to-normal (3F2N), an ultra-fast and highly accurate surface normal estimation

978-1-7281-7371-9/21/$31.00 ©2021 IEEE
Authorized licensed use limited to: University of Florida. Downloaded on January 11,2024 at 19:36:09 UTC from IEEE Xplore. Restrictions apply.

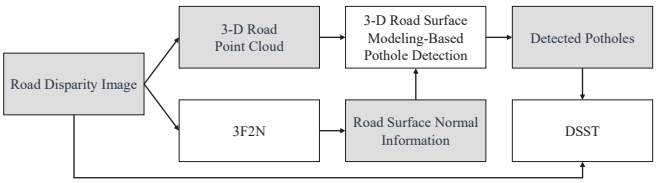

Fig. 1. Block diagram of the proposed road pothole detection and tracking system.

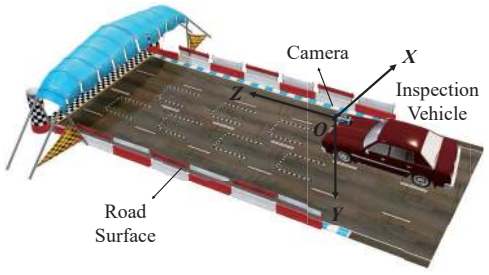

Fig. 2. Camera coordinate system. A stereo camera is mounted on the vehicle to capture road data.

algorithm. Furthermore, the discriminative scale space tracking (DSST) [40] algorithm is utilized to track the detected potholes in a sequence of successive video frames. The block diagram of the proposed system is depicted in Fig. 1. Extensive experimental results demonstrate the robustness of our proposed road pothole detection and tracking system.

D. Paper Outline

The remainder of this paper is organized as follows: Section II introduces our proposed scale-adaptive road pothole detection and tracking algorithm. Section III evaluates our proposed road pothole detection and tracking system. Finally, Section IV summarizes the paper and provides recommendations for future work.

II. System

A reconstructed 3-D road surface can be formulated as a quadratic surface [17]:

$$f(X,Z) = a_0 + a_1 X + a_2 Z + a_3 X^2 + a_4 Z^2 + a_5 XZ, \quad (1)$$

where $\boldsymbol{p} = (X;Y;Z)$ is a 3-D point on the road surface in the camera coordinate system (CCS), as illustrated in Fig. 2. $\boldsymbol{a} = (a_0;a_1;a_2;a_3;a_4;a_5)$ stores the quadratic surface coefficients. $\boldsymbol{a}$ can be estimated by minimizing:

$$E = \sum_{i=1}^{n} \Big(Y_i - f(X_i, Z_i) \Big)^2. \quad (2)$$

The optimal $\boldsymbol{a}$ can be obtained when:

$$\frac{\partial E}{\partial a_0} = \frac{\partial E}{\partial a_1} = \frac{\partial E}{\partial a_2} = \frac{\partial E}{\partial a_3} = \frac{\partial E}{\partial a_4} = \frac{\partial E}{\partial a_5} = 0. \quad (3)$$

which results in:

$$\boldsymbol{M}\boldsymbol{a} = \boldsymbol{q}, \quad (4)$$

where

$$\boldsymbol{M} = \begin{bmatrix} n & S_X & S_Z & S_{X^2} & S_{Z^2} & S_{XZ} \\ S_X & S_{X^2} & S_{XZ} & S_{X^3} & S_{XZ^2} & S_{ZX^2} \\ S_Z & S_{XZ} & S_{Z^2} & S_{ZX^2} & S_{Z^3} & S_{XZ^2} \\ S_{X^2} & S_{X^3} & S_{ZX^2} & S_{X^4} & S_{X^2Z^2} & S_{ZX^3} \\ S_{Z^2} & S_{XZ^2} & S_{Z^3} & S_{X^2Z^2} & S_{Z^4} & S_{XZ^3} \\ S_{XZ} & S_{X^2Z} & S_{XZ^2} & S_{X^3Z} & S_{XZ^3} & S_{X^2Z^2} \end{bmatrix}, \quad (5)$$

and

$$\boldsymbol{q} = (S_Y; S_{XY}; S_{YZ}; S_{YX^2}; S_{YZ^2}; S_{XYZ}). \quad (6)$$

S represents sum operation. For example, $S_{XZ^2} = \sum_1^n X_i {Z_i}^2$. (5) and (6) can be rewritten as:

$$\boldsymbol{M} = \boldsymbol{W}^\top \boldsymbol{W}, \quad (7)$$

and

$$\boldsymbol{q} = \boldsymbol{W}^\top \boldsymbol{y}, \quad (8)$$

where

$$\boldsymbol{W} = \begin{bmatrix} 1 & X_1 & Z_1 & {X_1}^2 & {Z_1}^2 & X_1 Z_1 \\ \vdots & \vdots & \vdots & \vdots & \vdots & \vdots \\ 1 & X_n & Z_n & {X_n}^2 & {Z_n}^2 & X_n Z_n \end{bmatrix}, \quad (9)$$

and

$$\boldsymbol{y} = (Y_1; Y_2; \cdots; Y_n). \quad (10)$$

Therefore, $\boldsymbol{a}$ has the following expression:

$$\boldsymbol{a} = \Big(\boldsymbol{W}^\top \boldsymbol{W} \Big)^{-1} \boldsymbol{W}^\top \boldsymbol{y}. \quad (11)$$

Following [17], we employ the RANSAC algorithm to iteratively update $\boldsymbol{a}$ with only a small proportion of 3-D road points, which can greatly reduce the effects caused by outliers. Moreover, [17] applies *PlanePCA* [41] to estimate the normal vectors of the 3-D points. Such normal vectors are then considered as part of the 3-D road surface modeling process to eliminate outliers. However, *PlanePCA* [41] is incredibly time-consuming, as it requires a selection of local points around each point in 3-D space in order to estimate the normal vector that is perpendicular to the interpolated planar surface. In this paper, we apply 3F2N [42] to acquire the surface normal information in real time. The surface normal $\boldsymbol{n}_i = (n_x; n_y; n_z)$ of $\boldsymbol{p}_i = (X_i; Y_i; Z_i)$ is formulated as [42]:

$$n_x = f_x \frac{\partial 1/Z_i}{\partial u}, \quad (12)$$

$$n_y = f_y \frac{\partial 1/Z_i}{\partial v}. \quad (13)$$

$$n_z = -\Phi \left\{ \frac{\Delta X_{ij} n_x + \Delta Y_{ij} n_y}{\Delta Z_{ij}} \right\}, \quad j = 1, \ldots, k, \quad (14)$$

where f_x and f_y are the horizontal and vertical focal lengths; Φ is a median filtering operation; $\Delta X_{ij} = X_i - X_j$, $\Delta Y_{ij} = Y_i - Y_j$, and $\Delta Z_{ij} = Z_i - Z_j$ can be computed given a neighboring

Authorized licensed use limited to: University of Florida. Downloaded on January 11,2024 at 19:36:09 UTC from IEEE Xplore. Restrictions apply.

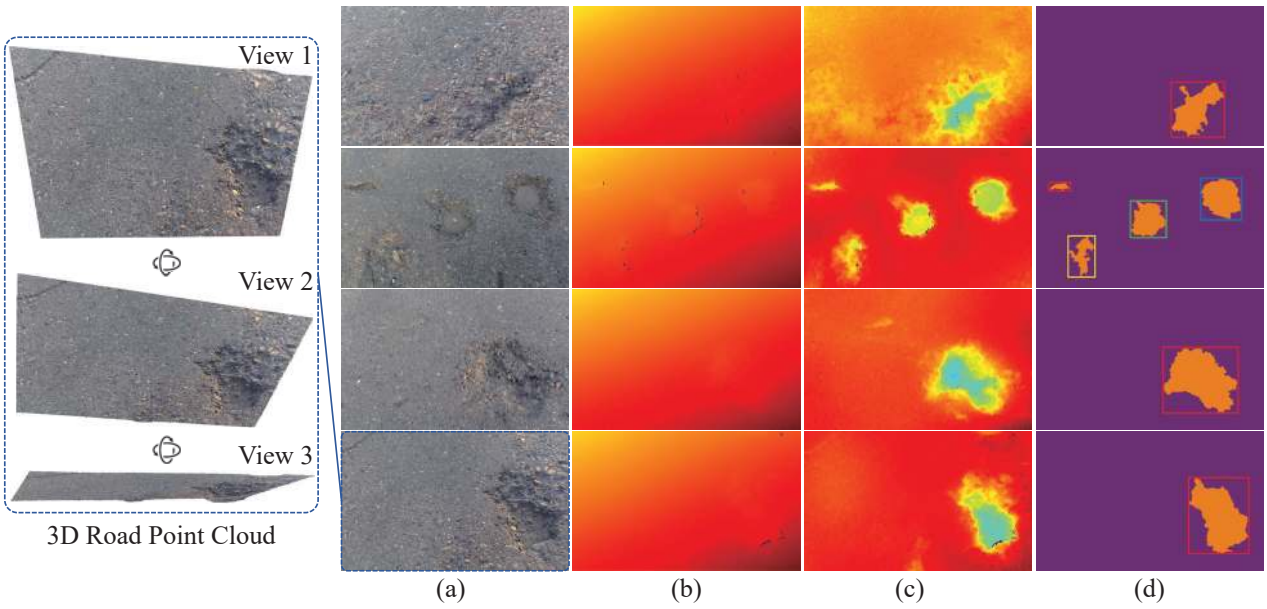

Fig. 3. Examples of the road pothole detection results: (a) RGB images; (b) disparity images; (c) transformed disparity images; (d) pothole detection results in pixel and instance levels.

point $\boldsymbol{q}_j = (X_j; Y_j; Z_j)$ of $\boldsymbol{p}_i$. The optimal surface normal vector of a given 3-D point $\boldsymbol{p}_i = (X_i; Y_i; Z_i)$ can be estimated using:

$$\hat{\boldsymbol{n}} = (a_1 + 2a_3X_i + a_5Z_i; -1; a_2 + 2a_4Z_i + a_5X_i). \quad (15)$$

By computing the difference (angle) between $\hat{\boldsymbol{n}}$ and $\boldsymbol{n}_i$:

$$\theta_i = \arccos\left(\frac{\hat{\boldsymbol{n}}_i \cdot \boldsymbol{n}_i}{||\hat{\boldsymbol{n}}_i||_2||\boldsymbol{n}_i||_2}\right), \quad (16)$$

the outliers can be determined, and they will not be considered into 3-D road surface modeling. Subsequently, we compare the difference between the actual and interpolated 3-D road surfaces. If $f(X_i, Z_i) - Y_i > t_r$, where t_r is the pothole detection threshold, $\boldsymbol{p}_i = (X_i; Y_i; Z_i)$ will be considered to be a 3-D point in the pothole areas. We also apply image post-processing algorithms, such as morphological operations, to refine the estimated pothole areas. Finally, different potholes are labeled using the connected component labeling algorithm.

Additionally, we employ DSST [40] to track the detected potholes in a sequence of successive video frames. Compared to some other state-of-the-art trackers such as High-speed tracking with kernelized correlation filters (KCF) [43], circulant structure of tracking (CSK) [44] and scale adaptive with multiple features tracker (SAMF) [45], the DSST performs better in terms of estimating the translation and size of the target in scenarios with scale variation [40]. Before tracking the detected potholes, we first utilize the disparity image processing algorithm proposed in [9] to transform our disparity image into a quasi bird's eye view:

$$\ell'(\boldsymbol{x}) = \ell(\boldsymbol{x}) - \kappa(v\cos\phi - u\sin\phi) - \kappa\varkappa + \delta, \quad (17)$$

where $\boldsymbol{x} = (u; v)$ is an image pixel, ℓ is the original disparity image, ℓ' is the transformed disparity image, ϕ is the stereo rig roll angle [46], κ and $\varkappa$ are two coefficients of the road disparity projection model [47], and δ is a constant set to ensure that the transformed disparities are non-negative. The expressions of κ and $\varkappa$ are as follows:

$$\varkappa = \frac{1}{c}\left(m\sum_{i=1}^{m}\ell(\boldsymbol{x}_i)w(\boldsymbol{x}_i,\phi) - \sum_{i=1}^{m}\ell(\boldsymbol{x}_i)\sum_{i=1}^{m}w(\boldsymbol{x}_i,\phi)\right), \quad (18)$$

$$\kappa = \frac{1}{\varkappa c}\left(\sum_{i=1}^{m}\ell(\boldsymbol{x}_i)\sum_{i=1}^{m}w(\boldsymbol{x}_i,\phi)^2 - \sum_{i=1}^{m}w(\boldsymbol{x}_i,\phi)\sum_{i=1}^{m}\ell(\boldsymbol{x}_i)w(\boldsymbol{x}_i,\phi)\right), \quad (19)$$

where

$$w(\boldsymbol{x},\phi) = v\cos\phi - u\sin\phi, \quad (20)$$

$$c = m\sum_{i=1}^{m}w(\boldsymbol{x}_i,\phi)^2 - \left(\sum_{i=1}^{m}w(\boldsymbol{x}_i,\phi)\right)^2. \quad (21)$$

The disparity transformation makes the road potholes highly distinguishable, improving the performance of road pothole tracking. Subsequently, we perform DSST [40] on our transformed disparity images to track the detected potholes. The performance of our proposed road pothole detection and tracking system will be evaluated in the next section.

III. Experimental Results

In this section, the performance of our proposed road pothole detection and tracking system is evaluated. This system is implemented in Matlab 2021b platform. The following subsections provide details on our used datasets and performance evaluation.

Authorized licensed use limited to: University of Florida. Downloaded on January 11,2024 at 19:36:09 UTC from IEEE Xplore. Restrictions apply.

Fig. 4. Pothole tracking results. The (same) potholes in different video frames are tracked with scale-adaptive bounding boxes.

A. Datasets

In our experiments, we first utilize the road pothole detection datasets[1] provided in [17] to evaluate the performance of our proposed road pothole detection system. Furthermore, we utilize the Bristol road pothole detection dataset, which contains two sequences of ∼2K successive stereo video frames, provided in [38] and [48] to evaluate the performance of road pothole tracking.

B. Performance Evaluation

Some examples of the detected road potholes in both pixel and instance levels are shown in Fig. 3. It can be seen that the road potholes can be successfully detected using our proposed 3-D road surface modeling algorithm, where different bounding box colors refer to different road potholes. Compared to [17], the 3-D road surface modeling process is approximately 2.7 times faster (on an Intel Core i7-8700K CPU using a single thread). The successful road pothole detection accuracy is over 98.7% as shown in Table I.

In addition, we also qualitatively evaluate the performance of DSST [40] for road pothole tracking on the transformed disparity images, as shown in Fig. 4. Readers can observe that DSST [40] performs robustly in terms of scale-adaptive road pothole tracking. Distant road potholes are localized by smaller bounding boxes, while nearby road potholes are localized by larger bounding boxes. Moreover, when part of road pothole is occluded by the vehicle, DSST [40] can still localize the road pothole robustly. Therefore, we believe DSST [40] is an effective tool that can be utilized for road pothole detection.

TABLE I
COMPARISON OF POTHOLE DETECTION ACCURACY.

Dataset	Method	Correct Detection	Incorrect Detection	Misdetection
Dataset 1	[48]	11	11	0
	proposed	22	0	0
Dataset 2	[48]	42	10	0
	proposed	51	1	0
Dataset 3	[48]	5	0	0
	proposed	5	0	0
Total	[48]	58	21	0
	proposed	78	1	0

IV. Conclusion and Future Work

In this paper we describe a robust 3-D road surface modeling algorithm based on our previously published work for road pothole detection, where the optimal surface normal vector of each 3-D point is efficiently estimated from the quadratic road surface modeling function. This greatly reduces the intensive computational complexity of the approach detailed in our previous work, where the normal vector of 3-D point is estimated by fitting a local planar surface using PlanePCA. Subsequently, the surface normal information was used to eliminate outliers for 3-D road surface modeling. By comparing the actual and modeled 3-D road surfaces, the 3-D pothole point clouds can be extracted. Finally, discriminative scale space tracking was applied to track the detected potholes in a sequence of successive video frames capturing transformed disparity information. Extensive experimental results demonstrated the robustness of our proposed road pothole detection and tracking system, where the achieved accuracy is around 99%, and the road potholes can be accurately tracked in different video frames with adaptive bounding box scales.

In the future, we plan to apply unsupervised learning with deep convolutional neural networks to detect/localize road potholes directly from either RGB or transformed disparity images. Furthermore, we also plan to develop a multi-target multi-camera tracking algorithm to track multiple potholes between stereo camera.

[1] https://github.com/ruirangerfan/stereo_pothole_datasets

References

[1] J. S. Miller *et al.*, "Distress identification manual for the long-term pavement performance program," United States. Federal Highway Ad-

Authorized licensed use limited to: University of Florida. Downloaded on January 11,2024 at 19:36:09 UTC from IEEE Xplore. Restrictions apply.

ministration., Tech. Rep., 2003.
[2] J. Fan *et al.*, "Multi-scale feature fusion: Learning better semantic segmentation for road pothole detection," in *The 2021 IEEE International Conference on Autonomous Systems (ICAS)*. IEEE, 2021.
[3] C. Koch *et al.*, "A review on computer vision based defect detection and condition assessment of concrete and asphalt civil infrastructure," *Advanced Engineering Informatics*, vol. 29, no. 2, pp. 196–210, 2015.
[4] R. Fan *et al.*, "Real-time dense stereo embedded in a uav for road inspection," in *2019 IEEE/CVF Conference on Computer Vision and Pattern Recognition Workshops*. IEEE, 2019, pp. 535–543.
[5] C. Koch *et al.*, "Automated pothole distress assessment using asphalt pavement video data," *Journal of Computing in Civil Engineering*, vol. 27, no. 4, pp. 370–378, 2013.
[6] R. Fan *et al.*, "Road crack detection using deep convolutional neural network and adaptive thresholding," in *2019 IEEE Intelligent Vehicles Symposium (IV)*. IEEE, 2019, pp. 474–479.
[7] J. Fan *et al.*, "Deep convolutional neural networks for road crack detection: Qualitative and quantitative comparisons," in *2021 IEEE International Conference on Imaging Systems and Techniques (IST)*. IEEE, 2021.
[8] P. Wang *et al.*, "Asphalt pavement pothole detection and segmentation based on wavelet energy field," *Mathematical Problems in Engineering*, vol. 2017, 2017.
[9] R. Fan *et al.*, "We learn better road pothole detection: from attention aggregation to adversarial domain adaptation," in *European Conference on Computer Vision*. Springer, 2020, pp. 285–300.
[10] X. Yu and E. Salari, "Pavement pothole detection and severity measurement using laser imaging," in *2011 IEEE International Conference on Electro/Information Technology*. IEEE, 2011, pp. 1–5.
[11] S. Mathavan, K. Kamal, and M. Rahman, "A review of three-dimensional imaging technologies for pavement distress detection and measurements," *IEEE Transactions on Intelligent Transportation Systems*, vol. 16, no. 5, pp. 2353–2362, 2015.
[12] R. Fan *et al.*, "Long-awaited next-generation road damage detection and localization system is finally here," in *2021 29th European Signal Processing Conference (EUSIPCO)*. IEEE, 2021, pp. 1–5.
[13] T. Kim and S.-K. Ryu, "Review and analysis of pothole detection methods," *Journal of Emerging Trends in Computing and Information Sciences*, vol. 5, no. 8, pp. 603–608, 2014.
[14] R. Fan *et al.*, "Real-time stereo vision for road surface 3-d reconstruction," in *2018 IEEE International Conference on Imaging Systems and Techniques (IST)*. IEEE, 2018, pp. 1–6.
[15] R. Fan, X. Ai, and N. Dahnoun, "Road surface 3d reconstruction based on dense subpixel disparity map estimation," *IEEE Transactions on Image Processing*, vol. 27, no. 6, pp. 3025–3035, 2018.
[16] R. Fan *et al.*, "Rethinking road surface 3-d reconstruction and pothole detection: From perspective transformation to disparity map segmentation," *IEEE Transactions on Cybernetics*, 2021.
[17] R. Fan, U. Ozgunalp, B. Hosking, M. Liu, and I. Pitas, "Pothole detection based on disparity transformation and road surface modeling," *IEEE Transactions on Image Processing*, vol. 29, pp. 897–908, 2019.
[18] R. Fan *et al.*, "Learning collision-free space detection from stereo images: Homography matrix brings better data augmentation," *IEEE/ASME Transactions on Mechatronics*, 2021.
[19] D. K. Dewangan and S. P. Sahu, "Potnet: Pothole detection for autonomous vehicle system using convolutional neural network," *Electronics Letters*, vol. 57, no. 2, pp. 53–56, 2021.
[20] W. Ye *et al.*, "Convolutional neural network for pothole detection in asphalt pavement," *Road materials and pavement design*, vol. 22, no. 1, pp. 42–58, 2021.
[21] H. Wang *et al.*, "Applying surface normal information in drivable area and road anomaly detection for ground mobile robots," in *2020 IEEE/RSJ International Conference on Intelligent Robots and Systems (IROS)*. IEEE, 2020, pp. 2706–2711.
[22] K. Bansal, K. Mittal, G. Ahuja, A. Singh, and S. S. Gill, "Deepbus: Machine learning based real time pothole detection system for smart transportation using iot," *Internet Technology Letters*, vol. 3, no. 3, p. e156, 2020.
[23] A. Kulkarni, N. Mhalgi, S. Gurnani, and N. Giri, "Pothole detection system using machine learning on android," *International Journal of Emerging Technology and Advanced Engineering*, vol. 4, no. 7, pp. 360–364, 2014.
[24] R. Fan, H. Wang, P. Cai, and M. Liu, "Sne-roadseg: Incorporating surface normal information into semantic segmentation for accurate freespace detection," in *European Conference on Computer Vision*. Springer, 2020, pp. 340–356.
[25] A. Kumar, D. J. Kalita, V. P. Singh *et al.*, "A modern pothole detection technique using deep learning," in *2nd International Conference on Data, Engineering and Applications (IDEA)*. IEEE, 2020, pp. 1–5.
[26] P. Ping *et al.*, "A deep learning approach for street pothole detection," in *2020 IEEE Sixth International Conference on Big Data Computing Service and Applications (BigDataService)*. IEEE, 2020, pp. 198–204.
[27] S. Li, C. Yuan, D. Liu, and H. Cai, "Integrated processing of image and gpr data for automated pothole detection," *Journal of computing in civil engineering*, vol. 30, no. 6, p. 04016015, 2016.
[28] R. Fan, M. J. Bocus, and N. Dahnoun, "A novel disparity transformation algorithm for road segmentation," *Information Processing Letters*, vol. 140, pp. 18–24, 2018.
[29] Y.-C. Tsai and A. Chatterjee, "Pothole detection and classification using 3d technology and watershed method," *Journal of Computing in Civil Engineering*, vol. 32, no. 2, p. 04017078, 2018.
[30] R. Fan and M. Liu, "Road damage detection based on unsupervised disparity map segmentation," *IEEE Transactions on Intelligent Transportation Systems*, 2019.
[31] C. Koch and I. Brilakis, "Pothole detection in asphalt pavement images," *Advanced Engineering Informatics*, vol. 25, no. 3, pp. 507–515, 2011.
[32] S.-K. Ryu, T. Kim, and Y.-R. Kim, "Image-based pothole detection system for its service and road management system," *Mathematical Problems in Engineering*, vol. 2015, 2015.
[33] R. Fan, "Real-time computer stereo vision for automotive applications," Ph.D. dissertation, University of Bristol, 2018.
[34] E. Buza, S. Omanovic, and A. Huseinovic, "Pothole detection with image processing and spectral clustering," in *Proceedings of the 2nd International Conference on Information Technology and Computer Networks*, vol. 810, 2013, p. 4853.
[35] M. R. Jahanshahi *et al.*, "Unsupervised approach for autonomous pavement-defect detection and quantification using an inexpensive depth sensor," *Journal of Computing in Civil Engineering*, vol. 27, no. 6, pp. 743–754, 2013.
[36] G. Jog *et al.*, "Pothole properties measurement through visual 2d recognition and 3d reconstruction," in *Computing in Civil Engineering (2012)*, 2012, pp. 553–560.
[37] J. W. Perng, C. H. Tai, C. H. Kuo, and L. S. Ma, "3d environment mapping and pothole detection for a mobile robot," in *Applied Mechanics and Materials*, vol. 431. Trans Tech Publ, 2013, pp. 287–292.
[38] U. Ozgunalp, "Vision based lane detection for intelligent vehicles," Ph.D. dissertation, University of Bristol, 2016.
[39] N. Otsu, "A threshold selection method from gray-level histograms," *IEEE transactions on systems, man, and cybernetics*, vol. 9, no. 1, pp. 62–66, 1979.
[40] M. Danelljan, G. Häger, F. S. Khan, and M. Felsberg, "Discriminative scale space tracking," *IEEE transactions on pattern analysis and machine intelligence*, vol. 39, no. 8, pp. 1561–1575, 2016.
[41] C. Wang *et al.*, "Comparison of local plane fitting methods for range data," in *Proceedings of the 2001 IEEE Computer Society Conference on Computer Vision and Pattern Recognition. CVPR 2001*, vol. 1. IEEE, 2001, pp. I–I.
[42] R. Fan *et al.*, "Three-filters-to-normal: An accurate and ultrafast surface normal estimator," *IEEE Robotics and Automation Letters*, vol. 6, no. 3, pp. 5405–5412, 2021.
[43] J. F. Henriques *et al.*, "High-speed tracking with kernelized correlation filters," *IEEE transactions on pattern analysis and machine intelligence*, vol. 37, no. 3, pp. 583–596, 2014.
[44] Henriques, João F *et al.*, "Exploiting the circulant structure of tracking-by-detection with kernels," in *European conference on computer vision*. Springer, 2012, pp. 702–715.
[45] Y. Li and J. Zhu, "A scale adaptive kernel correlation filter tracker with feature integration," in *European conference on computer vision*. Springer, 2014, pp. 254–265.
[46] N. Vinogradov *et al.*, "Implementation of stereo rig roll angle estimation on a tms320c6678 dsp," in *2020 9th Mediterranean Conference on Embedded Computing (MECO)*. IEEE, 2020, pp. 1–4.
[47] H. Wang *et al.*, "Dynamic fusion module evolves drivable area and road anomaly detection: A benchmark and algorithms," *IEEE transactions on cybernetics*, 2021.
[48] Z. Zhang, "Advanced stereo vision disparity calculation and obstacle analysis for intelligent vehicles," Ph.D. dissertation, University of Bristol, 2013.

Authorized licensed use limited to: University of Florida. Downloaded on January 11,2024 at 19:36:09 UTC from IEEE Xplore. Restrictions apply.